View metadata, citation and similar papers at core.ac.uk

brought to you by CORE

provided by NERC Open Research Archive

Article (refereed) - postprint

Read, Daniel S.; Whiteley, Andrew S. 2015. **Chemical fixation methods for Raman spectroscopy-based analysis of bacteria**.

Copyright © 2014 Elsevier B.V.

This version available http://nora.nerc.ac.uk/509290/

NERC has developed NORA to enable users to access research outputs wholly or partially funded by NERC. Copyright and other rights for material on this site are retained by the rights owners. Users should read the terms and conditions of use of this material at
http://nora.nerc.ac.uk/policies.html#access

NOTICE: this is the author's version of a work that was accepted for publication in *Journal of Microbiological Methods*. Changes resulting from the publishing process, such as peer review, editing, corrections, structural formatting, and other quality control mechanisms may not be reflected in this document. Changes may have been made to this work since it was submitted for publication. A definitive version was subsequently published in *Journal of Microbiological Methods* (2015), 109. 79-83.
10.1016/j.mimet.2014.12.008

www.elsevier.com/

Contact CEH NORA team at
noraceh@ceh.ac.uk

The NERC and CEH trademarks and logos ('the Trademarks') are registered trademarks of NERC in the UK and other countries, and may not be used without the prior written consent of the Trademark owner.

1 # Chemical fixation methods for Raman spectroscopy-based analysis of
2 # bacteria

3

4 Daniel S. Read[1] and Andrew S. Whiteley[2.]

5

6 [1]Centre for Ecology & Hydrology, Benson Lane, Crowmarsh Gifford, Wallingford, OX10 8BB,
7 UK.

8 [2]School of Earth and Environment, The University of Western Australia, Stirling Highway,
9 Crawley, Western Australia. 6065.

10

11 Correspondance: Dr D.S. Read, E-mail : dasr@ceh.ac.uk

12

13

14 Keywords: Raman spectroscopy, fixation, phenotype, bacteria.

15

ABSTRACT

Preservation of biological samples for downstream analysis is important for analytical methods that measure the biochemical composition of a sample. One such method, Raman microspectroscopy, is commonly used as a rapid phenotypic technique to measure biomolecular composition for the purposes of identification and discrimination of species and strains of bacteria, as well as investigating physiological responses to external stressors and the uptake of stable isotope-labelled substrates in single cells. This study examines the influence of a number of common chemical fixation and inactivation methods on the Raman spectrum of six species of bacteria. Modifications to the Raman-phenotype caused by fixation were compared to unfixed control samples using difference spectra and Principal Components Analysis (PCA). Additionally, the effect of fixation on the ability to accurately classify bacterial species using their Raman phenotype was determined. The results showed that common fixatives such as glutaraldehyde and ethanol cause significant changes to the Raman spectra of bacteria, whereas formaldehyde and sodium azide were better at preserving spectral features.

31 INTRODUCTION

32 Raman microspectroscopy is a method commonly used for the phenotypic measurement of
33 biological samples, ranging from individual cells to complex structures such as biofilms and
34 tissues (Huang et al., 2010, Schuster et al., 2000). Measurement of the inelastic scattering of
35 light (Raman scattering) can be used to non-destructively determine the molecular
36 composition of a biological sample (Schie and Huser, 2013). The Raman spectrum can provide
37 a spectroscopic fingerprint that can measure the molecular composition of cells, comprising
38 major biological molecules including proteins, amino acids, lipids, polysaccharides, nucleic
39 acids and nucleobases (Huang, Li, Jarvis, Goodacre and Banwart, 2010).

40

41 One of the most frequent applications of Raman spectroscopy in microbiology is to measure
42 the cellular composition (the phenotype) for the purposes of species/strain identification.
43 This approach has previously been used to identify and discriminate between species and
44 strains of fungi (De Gussem et al., 2007), algae (Huang et al., 2010), viruses (Driskell et al.,
45 2010) and most frequently bacteria (Palchaudhuri et al., 2011, Read et al., 2013). As well as a
46 rapid identification tool, Raman has been used to examine the phenotypic and physiological
47 changes that occur with exposure to stressors in the form of pollutants such as ionic metals
48 (Walter et al., 2012), metal nanoparticles (Cherchi et al., 2011), organic pollutants (Daniel et
49 al., 2008, Singer et al., 2005), antibiotics (Escoriza et al., 2007), and pharmaceuticals (Wharfe
50 et al., 2010). Raman has also been used to measure the concentration and spatial distribution
51 of cellular metabolites such as algal lipids (Wu et al., 2011) and pigments such as carotenoids
52 (Tao et al., 2011) and chlorophyll (Huang, Beal, Cai, Ruoff and Terentjev, 2010). Finally, there
53 is an emerging application applying Raman microspectroscopy as a tool for stable isotope

54 probing (SIP) to monitor substrate utilisation by single bacterial cells (Huang et al., 2004,
55 Huang et al., 2007).
56
57 As with all analytical techniques that measure phenotypic characteristics (such as proteomics,
58 metabolomics and lipidomics), methods for sample handling and preservation of samples for
59 later analysis are of critical importance. As Raman spectroscopy measures the molecular
60 composition of the cell, it is important to use preservation methods that cause minimal
61 changes to the composition and arrangement of molecules that make up the Raman
62 fingerprint. Unless cells are suitably fixed, autolysis by intracellular enzymes can denature
63 proteins and dephosphorylate mononucleotides, phospholipids and proteins (Gazi et al.,
64 2005), potentially altering the Raman fingerprint.
65
66 Previous work examining the role of sample handling and preservation techniques on the
67 Raman spectra of eukaryotic tissues have highlighted method-dependant spectral alterations.
68 These include the effects of ethanol and glycerol on bone samples (Yeni et al., 2006), snap
69 freezing in liquid nitrogen on porcine prostate tissue (Candefjord et al., 2009), formaldehyde
70 or methanol fixation in leukaemia cells lines (Chan et al., 2009), formaldehyde, desiccation
71 and air drying on human cell lines (Mariani et al., 2009), desiccation on human embryonic
72 stem cells (Konorov et al., 2011) and formalin or Carnoy's fixative on human cell lines (Meade
73 et al., 2010). There have been studies examining fixation and inactivation induced effects on
74 bacterial spectra, but these have focussed specifically on purple non-sulfur bacteria
75 (Kniggendorf et al., 2011) and endospore forming species (Stockel et al., 2010).
76

77 The objective of the current study was to investigate the influence of a number of common
78 chemical fixatives on the Raman spectra of species of bacteria representing a range of
79 different Raman phenotypes. Here we have examined the effect that each fixative has on the
80 Raman spectra of six species of bacteria, followed by an examination of the influence of each
81 fixative on the ability to correctly identify each bacterial species based on their Raman
82 spectra.

83

84 MATERIALS AND METHODS

85 Bacterial isolates and culturing

86 Six bacterial species, selected to represent a range of differing phenotypes, were purchased
87 from Leibniz Institute DSMZ-German Collection of Microorganisms and Cell Cultures
88 (Germany). These were; *Escherichia coli* (ATCC 1775), *Bacillus subtilis* subsp. *subtilis* (ATCC
89 6051), *Pseudomonas fluorescens* (ATCC 13525), *Pseudomonas aeruginosa* (ATCC 10145),
90 *Micrococcus luteus* (ATCC 4698), and *Janthinobacterium lividum* (ATCC 12473). All strains
91 were checked for purity by streaking onto LB agar (Sigma Aldrich, UK) and cultured overnight
92 at 28 °C. Single colonies were picked and sub cultured in 5 ml of LB broth (Sigma, UK) with
93 shaking at 180 rpm. Each culture was diluted to an OD_{600} of 0.5 and used to inoculate 180 ml
94 of LB broth for each treatment and again grown overnight (16 h) at 28 °C with shaking at 180
95 rpm. The cell suspension was well mixed, and divided into six aliquots of 30 ml, one for each
96 of the fixation methods and then further divided into three aliquots of 10 ml to provide
97 technical fixation replicates. To remove the influence of the culture media on the fixation
98 methods, each cell suspension was centrifuged for 5 min at 5000 g, the supernatant removed
99 using a pipette and cells re-suspended in ice cold x1 PBS.

100

101 Fixation and sample handling

102 Five methods of chemical cell fixation were compared, including fixation in 70/30 (vol:vol) mix
103 of ethanol (EtOH) and molecular grade water, a solution of 2.0% neutral buffered
104 formaldehyde (CH_2O) made fresh from paraformaldehyde (adjusted to pH 7.2), a solution of
105 1.0% glutaraldehyde ($CH_2(CH_2CHO)_2$), a solution of 1.0% Formaldehyde and 0.05%
106 glutaraldehyde, and finally a solution of 10% (w/v) Sodium azide (NaN_3). All chemicals were
107 purchased from Sigma-Adrich, UK. Cell pellets were re-suspended in each fixative and allowed
108 to fix for 1 h at room temperature before the being washed, pelleted and re-suspended in ice
109 cold MQ H_2O three times as before. The supernatant was removed a final time using a pipette
110 to leave a cell pellet. The control sample consisted of unfixed cells frozen immediately after
111 washing. The samples were then prepared for analysis by Raman spectroscopy by spotting 10
112 µl of the cell pellet from each replicate and treatment onto spectroscopy grade CaF_2 slide
113 (Crystran, UK) and dried in a laboratory desiccator at room temperature for 30 minutes.
114

115 Raman microspectroscopy

116 Raman spectroscopy was conducted on a Horiba LabRAM HR800 Raman microspectrometer
117 (Horiba Scientific, UK) equipped with an Olympus BX-41 microscope and an Andor
118 electronically cooled CCD detector. The dried cell mass was visually focused on using a
119 100x/0.9 numerical-aperture Olympus M Plan air objective and a CCD camera, viewed on
120 LabSpec v5. The samples were illuminated with a 532-nm Nd:YAG laser and the incident laser
121 power was adjusted to 5-8 mW. The signal was optimized by adjusting the laser focus using
122 the real-time readout of the Raman signal, before acquiring the spectrum between 211 cm^{-1}
123 and 1894 cm^{-1}, with 1,022 data points (~1.5 cm^{-1} per point). Each spectrum consisted of two
124 averaged 30 s exposures. Cosmic spikes were automatically removed using LabSpec v5

125 software (Horiba Scientific, UK). Raman spectra were collected from 4-8 spatially offset points
126 within each dried bacterial spot for each replicate, to give a total of 12-24 spectra per
127 treatment.
128
129 Data analysis
130 Raw spectra were concatenated to between 400 cm^{-1} and 1800 cm^{-1} wavenumbers, and the
131 data normalized (area under spectra to 100 units) using LabSpec V5. The data analysis had
132 two main objectives; firstly to examine the relative influence of fixation on the Raman spectra
133 of the different bacterial species. Difference spectra were generated by subtracting the
134 average spectra of each treatment from the average control spectra. Differences in the
135 structure and shape of the treatment vs. the control are highlighted in deviations from the
136 zero line. To further explore fixation-induced changes in spectral composition, Principle
137 Components Analysis (PCA) was used to examine the relationships of all the treatments for
138 each spectrum. PCA was conducted in the R programming environment (R Core Team, 2013)
139 using the package "ChemometricsWithR" (Wehrens, 2012). The second objective was to
140 examine the influence of fixation on the ability to accurately discriminate between bacterial
141 species using their Raman spectra. Hierarchical Cluster Analysis (HCA) in R was used to create
142 a dendrogram for each treatment, showing unsupervised clustering of the spectra replicates
143 for each strain. Additionally, the accuracy of species discrimination was assessed using Linear
144 Discriminant Analysis (LDA) in the R package "MASS" (Venables and Ripley, 2002) and the
145 apparent error rate visualized and assessed using the KlaR package (Weihs et al., 2005).
146
147 RESULTS AND DISCUSSION

148 Due to very high levels of autoflorescence, it was not possible to collect a spectrum from *J.*
149 *lividu*m fixed with a formaldehyde and glutaraldehyde solution, so these data were excluded
150 from further analysis. Figure 1 shows representative Raman spectra from unfixed samples of
151 each of the six species. Whilst the overall structure and composition of the spectra are broadly
152 similar, there are some differences caused by variation in the fluorescence background for
153 each species. Although there was a concordance in terms of the presence/absence of specific
154 peaks found across species, some Raman peaks were found to be unique to particular species
155 and not others (Supplementary Table 1). In particular *M. luteus* had peaks associated with
156 carotene–like pigments at 1157 and 1527 cm^{-1} that are absent in the other species. The peaks
157 identified in this study are in agreement with previous studies (Huang, Li, Jarvis, Goodacre
158 and Banwart, 2010) and represent the major biomolecules found in bacterial cells, including
159 proteins, amino acids, lipids, carbohydrates, nucleic acids and nucleobases (Supplementary
160 Table 1).
161
162 Fixation with EtOH (and other solvents) are used for denaturing fixation and cause rapid
163 dehydration of the cells and additionally may solubilize membrane lipids (Woods and Ellis,
164 1994). Ethanol fixation caused large changes in the overall composition of the bacterial
165 Raman spectra compared to the unfixed control, with an increase in peak height relative to
166 unfixed controls. This change is possibly due to a reduction in background fluorescence
167 caused by soluble fluorescent biomolecules being washed away during fixation. A mix of
168 0.25% ammonia and 70% ethanol has previously been shown to reduce autofluorescence in
169 archival bone marrow sections, possibly through the dissolution of negatively charged lipid
170 derivatives, phenols or polypenols and degradation of weak esters by hydrolysis (Baschong et
171 al., 2001). The Raman peak at 749 cm^{-1} assigned to cytochrome *c* was generally reduced in

172 intensity by EtOH fixation across all species other than *E. coli*. However the effects of fixation
173 are inconsistent; both *P. aeruginosa* and *B. subtilis* show an increase in intensity in the second
174 half of the spectra when fixed with ethanol, whereas *E. coli*, J*. lividum*, *M. luteus* and *P.*
175 *fluorescens* were largely reduced in intensity. Over all, EtOH fixation caused significant
176 changes in the bacterial phenotype as none of the fixed samples clustered in close proximity
177 to the control (Figure 3).
178
179 Fixation with glutaraldehyde resulted in major changes to the structure of the Raman spectra
180 in all species, shown by the deviation of the treatment spectra from the control line in Figure
181 2. This was caused by increased levels of background fluorescence, obscuring the appearance
182 of informative Raman peaks. Both glutaraldehyde and formaldehyde are additive fixation
183 solutions (also called cross-linking fixations) (St-Laurent et al., 2006), and work by forming
184 covalent cross-links between amine residues in proteins (Meade, Clarke, Draux, Sockalingum,
185 Manfait, Lyng and Byrne, 2010). The generation of high levels of autofluorescence in
186 glutaraldehyde fixed tissues has been observed previously, and is has been postulated that
187 this is caused by the presence of dialdehyde groups (Lee *et al.*, 2013). The mix of
188 formaldehyde and glutaraldehyde caused inconsistent results, where in some species it
189 resulted in high levels of autofluorescence (*E. coli*, *J. lividum*, and *P. aeruginosa*) and in others
190 (*B. subtilis*, *M. luteus* and *P. fluorescens*) relatively small changes. This was confirmed in the
191 PCA plots, where gluteraldehyde was shown to cause significant changes to the Raman
192 spectrum of all the species tested when compared to the control (Figure 3). This was also the
193 case for the NBF + glutaraldehyde mix, except for *B. subtilis* where the points were the close
194 to the control spectra (Figure 3).
195

196 Unlike fixation with gluteraldehyde, cells preserved with formaldehyde alone appeared to be
197 relatively conserved in terms of spectral/phenotypic modifications, with the main changes
198 being associated with a reduction in the intensity of the peak at 749 cm^{-1}, assigned to
199 cytochrome *c*. The largest changes caused by fixation with formaldehyde were observed in
200 *M. luteus* where a small increase in peak intensity across the spectral range was observed
201 when compared to the control (Figure 2), and *B. subtilis*, where the overall shape of the
202 spectra was changed, possibly by increased autofluorescence. Points associated with
203 formaldehyde fixed samples generally clustered in close proximity to the control samples in
204 the PCA plots (Figure 3).
205
206 Finally, fixation with Sodium azide (NaN_3) resulted in conserved phenotypic changes when
207 compared to the unfixed control, as shown by the relatively small deviation from the zero line
208 in the subtraction plots (Figure 2). This is true for all species except *M. luteus*, which showed
209 reductions in the intensity of peaks at 1154 cm^{-1} and 1527 cm^{-1} which have previously been
210 assigned to the vibration modes of carotene (Scholtes-Timmerman et al., 2009). NaN_3 binds
211 to heme-iron found in cytochrome oxidase and catalase, effectively leading to chemical
212 asphyxiation (Lichstein and Soule, 1944). Similar to the formaldehyde fixed samples, points
213 associated with NaN_3 fixed samples generally clustered in close proximity to the control
214 samples in the PCA plots (Figure 3).
215
216 Hierarchical Cluster Analysis (HCA) and Linear Discriminant Analysis (LDA) were used to assess
217 the overall performance of the fixatives when used in Raman spectroscopy-based
218 classification studies. Changes in the bacterial phenotype upon fixation may alter the ability
219 to correctly classify different species of bacteria using Raman spectroscopy. For the unfixed

220 samples using both HCA and LDA all six species were assigned to separate clusters, with no
221 misclassifications (Figure 4 and Figure S1). Fixation with NaN_3 was the only other method able
222 to achieve this, with all species clearly located in different clusters. All other fixation methods
223 failed to produce a perfect classification, with varying degrees of misclassification (Figure S1).
224 However, fixation with NaN_3 caused considerable changes in the relationships between the
225 groups as shown by the positioning of the cluster branches (Figure 4). For example, where
226 the *E. coli* spectra formed a distinct outgroup on the unfixed cluster plot, this was joined by
227 *B. subtilis* spectra in the NaN_3 fixed plot. This reordering of spectral similarity is not of great
228 importance if the only aim it to assign spectra to the correct group. However, if the intention
229 is to infer something about the similarity of the bacterial phenotypes, great care needs to be
230 taken when using any fixation method.
231
232 CONCLUSIONS
233 All fixatives investigated caused changes to the Raman spectroscopy measured phenotype of
234 the six bacterial species used in this study. However, fixation with NaN_3 appeared to be the
235 most conserved in terms of deviation of the spectra from the control samples and the ability
236 to retain a high degree of classification success. One aspect not investigated in this study was
237 the potential effects of longer term storage of samples when unfixed or fixed, both at room
238 temperature and frozen. The main aim of fixation is to prevent cellular processes and cell
239 replication from continuing during storage. It is possible that in cases where inactivation of
240 cells and fixation is not needed, freezing samples at -80 °C or colder will be appropriate.
241 However, further work is needed to determine the impact of freezing on the preservation of
242 cells, especially over longer term storage. For pathogenic species of bacteria, preservation
243 and inactivation using a fixative may be necessary from a safety point of view (Stockel,

244 Schumacher, Meisel, Elschner, Rosch and Popp, 2010). If this is the case, Sodium azide is an

245 appropriate fixative in terms of preserving Raman phenotypic characteristics.

246

247 ACKNOWLEDGEMENTS

248 This work NE/I001093/1 was funded with support from the Natural Environment Research

249 Council's (NERC) Technology Proof of Concept (TPOC) programme.

250 REFERENCES

251 Baschong, W., Suetterlin, R., Laeng, R.H., 2001. Control of autofluorescence of archival
252 formaldehyde-fixed, paraffin-embedded tissue in confocal laser scanning microscopy (CLSM).
253 J Histochem Cytochem. 49, 1565-1571.

254 Candefjord, S., Ramser, K., Lindahl, O.A., 2009. Effects of snap-freezing and near-infrared laser
255 illumination on porcine prostate tissue as measured by Raman spectroscopy. Analyst. 134,
256 1815-1821.

257 Chan, J.W., Taylor, D.S., Thompson, D.L., 2009. The effect of cell fixation on the discrimination
258 of normal and leukemia cells with laser tweezers Raman spectroscopy. Biopolymers. 91, 132-
259 139.

260 Cherchi, C., Chernenko, T., Diem, M., Gu, A.Z., 2011. Impact of nano titanium dioxide exposure
261 on cellular structure of *Anabaena variabilis* and evidence of internalization. Environ Toxicol
262 Chem. 30, 861-869.

263 Daniel, P., Picart, P., Bendriaa, L., Sockalingum, G.D., Adt, I., Charrier, T., Durand, M.J., Ergan,
264 F., Manfait, M., Thouand, G., 2008. Effects of toxic organotin compounds on bacteria
265 investigated by micro-raman spectroscopy. Spectrosc Lett. 41, 19-28.

266 De Gussem, K., Vandenabeele, P., Verbeken, A., Moens, L., 2007. Chemotaxonomical
267 identification of spores of macrofungi: possibilities of Raman spectroscopy. Anal Bioanal
268 Chem. 387, 2823-2832.

269 Driskell, J.D., Zhu, Y., Kirkwood, C.D., Zhao, Y., Dluhy, R.A., Tripp, R.A., 2010. Rapid and
270 sensitive detection of rotavirus molecular signatures using surface enhanced Raman
271 spectroscopy. Plos One. 5, e10222.

272 Escoriza, M.F., VanBriesen, J.M., Stewart, S., Maier, J., 2007. Raman spectroscopic
273 discrimination of cell response to chemical and physical inactivation. Appl Spectrosc. 61, 812-
274 823.
275 Gazi, E., Dwyer, J., Lockyer, N.P., Miyan, J., Gardner, P., Hart, C., Brown, M., Clarke, N.W.,
276 2005. Fixation protocols for subcellular imaging by synchrotron-based Fourier transform
277 infrared microspectroscopy. Biopolymers. 77, 18-30.
278 Huang, W.E., Griffiths, R.I., Thompson, I.P., Bailey, M.J., Whiteley, A.S., 2004. Raman
279 microscopic analysis of single microbial cells. Anal Chem. 76, 4452-4458.
280 Huang, W.E., Li, M., Jarvis, R.M., Goodacre, R., Banwart, S.A., 2010. Shining light on the
281 microbial world the application of Raman microspectroscopy. Adv Appl Microbiol. 70, 153-
282 186.
283 Huang, W.E., Stoecker, K., Griffiths, R., Newbold, L., Daims, H., Whiteley, A.S., Wagner, M.,
284 2007. Raman-FISH: combining stable-isotope Raman spectroscopy and fluorescence in situ
285 hybridization for the single cell analysis of identity and function. Environ Microbiol. 9, 1878-
286 1889.
287 Huang, Y.Y., Beal, C.M., Cai, W.W., Ruoff, R.S., Terentjev, E.M., 2010. Micro-Raman
288 spectroscopy of algae: composition analysis and fluorescence background behavior.
289 Biotechnol Bioeng. 105, 889-898.
290 Kniggendorf, A.K., Gaul, T.W., Meinhardt-Wollweber, M., 2011. Effects of ethanol,
291 formaldehyde, and gentle heat fixation in confocal resonance Raman microscopy of purple
292 nonsulfur bacteria. Microsc Res Tech. 74, 177-183.
293 Konorov, S.O., Schulze, H.G., Piret, J.M., Turner, R.F.B., Blades, M.W., 2011. Evidence of
294 marked glycogen variations in the characteristic Raman signatures of human embryonic stem
295 cells. J Raman Spectrosc. 42, 1135-1141.

296 Lichstein, H.C., Soule, M.H., 1944. Studies of the effect of sodium azide on microbic growth
297 and respiration: IV. The effect of sodium azide on glucose fermentation and lactic acid
298 production by Streptococci and Lactobacilli. Journal of Bacteriology. 47, 253-257.
299 Mariani, M.M., Lampen, P., Popp, J., Wood, B.R., Deckert, V., 2009. Impact of fixation on in
300 vitro cell culture lines monitored with Raman spectroscopy. Analyst. 134, 1154-1161.
301 Meade, A.D., Clarke, C., Draux, F., Sockalingum, G.D., Manfait, M., Lyng, F.M., Byrne, H.J.,
302 2010. Studies of chemical fixation effects in human cell lines using Raman microspectroscopy.
303 Anal Bioanal Chem. 396, 1781-1791.
304 Palchaudhuri, S., Rehse, S.J., Hamasha, K., Syed, T., Kurtovic, E., Kurtovic, E., Stenger, J., 2011.
305 Raman spectroscopy of xylitol uptake and metabolism in Gram-positive and Gram-negative
306 bacteria. Appl Environ Microbiol. 77, 131-137.
307 R Core Team, 2013. R: A language and environment for statistical computing. , R Foundation
308 for Statistical Computing Vienna, Austria.
309 Read, D.S., Woodcock, D.J., Strachan, N.J., Forbes, K.J., Colles, F.M., Maiden, M.C., Clifton-
310 Hadley, F., Ridley, A., Vidal, A., Rodgers, J., Whiteley, A.S., Sheppard, S.K., 2013. Evidence for
311 phenotypic plasticity among multihost *Campylobacter jejuni* and *C. coli* lineages, obtained
312 using ribosomal multilocus sequence typing and Raman spectroscopy. Appl Environ Microbiol.
313 79, 965-973.
314 Schie, I.W., Huser, T., 2013. Methods and applications of Raman microspectroscopy to single-
315 cell analysis. Appl Spectrosc. 67, 813-828.
316 Scholtes-Timmerman, M., Willemse-Erix, H., Schut, T.B., van Belkum, A., Puppels, G.,
317 Maquelin, K., 2009. A novel approach to correct variations in Raman spectra due to photo-
318 bleachable cellular components. Analyst. 134, 387-393.

319 Schuster, K.C., Urlaub, E., Gapes, J.R., 2000. Single-cell analysis of bacteria by Raman
320 microscopy: spectral information on the chemical composition of cells and on the
321 heterogeneity in a culture. J Microbiol Methods. 42, 29-38.
322 Singer, A.C., Huang, W.E., Helm, J., Thompson, I.P., 2005. Insight into pollutant bioavailability
323 and toxicity using Raman confocal microscopy. J Microbiol Methods. 60, 417-422.
324 St-Laurent, J., Boulay, M.E., Prince, P., Bissonnette, E., Boulet, L.P., 2006. Comparison of cell
325 fixation methods of induced sputum specimens: an immunocytochemical analysis. J Immunol
326 Methods. 308, 36-42.
327 Stockel, S., Schumacher, W., Meisel, S., Elschner, M., Rosch, P., Popp, J., 2010. Raman
328 spectroscopy-compatible inactivation method for pathogenic endospores. Appl Environ
329 Microbiol. 76, 2895-2907.
330 Tao, Z., Wang, G., Xu, X., Yuan, Y., Wang, X., Li, Y., 2011. Monitoring and rapid quantification
331 of total carotenoids in *Rhodotorula glutinis* cells using laser tweezers Raman spectroscopy.
332 Fems Microbiol Lett. 314, 42-48.
333 Venables, W.N., Ripley, B.D., 2002. Modern Applied Statistics with S, Springer.
334 Walter, A., Kuhri, S., Reinicke, M., Bocklitz, T., Schumacher, W., Rosch, P., Merten, D., Buchel,
335 G., Kothe, E., Popp, J., 2012. Raman spectroscopic detection of Nickel impact on single
336 Streptomyces cells - possible bioindicators for heavy metal contamination. J Raman Spectrosc.
337 43, 1058-1064.
338 Wehrens, R., 2012. Chemometrics With R: Multivariate Data Analysis in the Natural Sciences
339 and Life Sciences.
340 Weihs, C., Ligges, U., Luebke, K., Raabe, N., 2005. klaR Analyzing German Business Cycles. In:
341 D. Baier, R. Decker, L. Schmidt-Thieme (Eds.), Data Analysis and Decision Support, Springer
342 Berlin Heidelberg, pp. 335-343.

343 Wharfe, E.S., Winder, C.L., Jarvis, R.M., Goodacre, R., 2010. Monitoring the effects of chiral
344 pharmaceuticals on aquatic microorganisms by metabolic fingerprinting. Appl Environ
345 Microbiol. 76, 2075-2085.
346 Woods, A.E., Ellis, R.C., 1994. Laboratory Histopathology: A Complete Reference, Churchill
347 Livingstone.
348 Wu, H., Volponi, J.V., Oliver, A.E., Parikh, A.N., Simmons, B.A., Singh, S., 2011. In vivo
349 lipidomics using single-cell Raman spectroscopy. Proc Natl Acad Sci U S A. 108, 3809-3814.
350 Yeni, Y.N., Yerramshetty, J., Akkus, O., Pechey, C., Les, C.M., 2006. Effect of fixation and
351 embedding on Raman spectroscopic analysis of bone tissue. Calcif Tissue Int. 78, 363-371.

352 FIGURE LEGENDS

353

354 Figure 1. Representative Raman spectra for each species of bacteria used in this study;
355 *Escherichia coli* (Ec), *Janthinobacterium lividum* (Jl), *Pseudomonas aeruginosa* (Pa), *Bacillus*
356 *subtilis* (Bs), *Micrococcus luteus* (Ml) and *Pseudomonas fluorescens* (Pf). Major peaks are
357 highlighted with grey bars.

358

359 Figure 2. Difference spectra (average control spectra minus the average treatment spectra)
360 for each species of bacteria used in this study; *Escherichia coli* (Ec); *Janthinobacterium lividum*
361 (Jl), *Pseudomonas aeruginosa* (Pa), *Bacillus subtilis* (Bs), *Micrococcus luteus* (Ml) and
362 *Pseudomonas fluorescens* (Pf) for each of the five fixation treatments used; 70% ethanol
363 (EtOH), Glutaraldehyde (Glut), Sodium azide (NaN_3), Formaldehyde (Form), Formaldehyde
364 and Glutaraldehyde (Form+Glut).

365

366 Figure 3. Principle Component Analysis (PCA) plots showing the relationship between the
367 control and fixation treatment spectra for each of the six species of bacteria used in this study;
368 *Escherichia coli* (A), *Janthinobacterium lividum* (B), *Pseudomonas aeruginosa* (C), *Bacillus*
369 *subtilis* (D), *Micrococcus luteus* (E), *Pseudomonas fluorescens* (F).

370

371 Figure 4. Hierarchical Cluster Analysis (HCA) plots showing the relationship between Raman
372 derived phenotypes from each fixation treatment; Unfixed (A), 70% Ethanol (B),
373 Glutaraldehyde (C), Sodium azide (D), Formaldehyde (E), Formaldehyde and Glutaraldehyde
374 (F). Colors represent species of bacteria used in this study, including *Escherichia coli* (Ec - blue),

375 *Janthinobacterium lividum* (Jl – green), *Pseudomonas aeruginosa* (Pa - yellow), *Bacillus subtilis*

376 (Bs - red), *Micrococcus luteus* (Ml - orange), *Pseudomonas fluorescens* (Pf - purple).

377

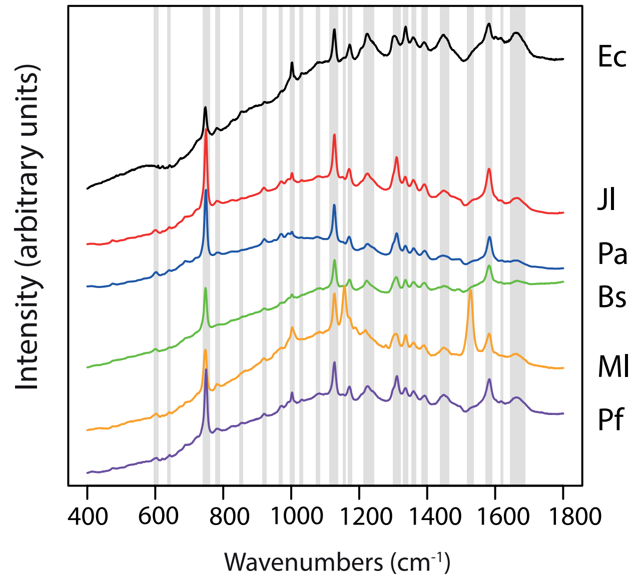

Intensity (arbitrary units)
Ec
Jl
Pa
Bs
Ml
Pf
400
600
800
1000
1200
1400
1600
1800
Wavenumbers (cm-1)

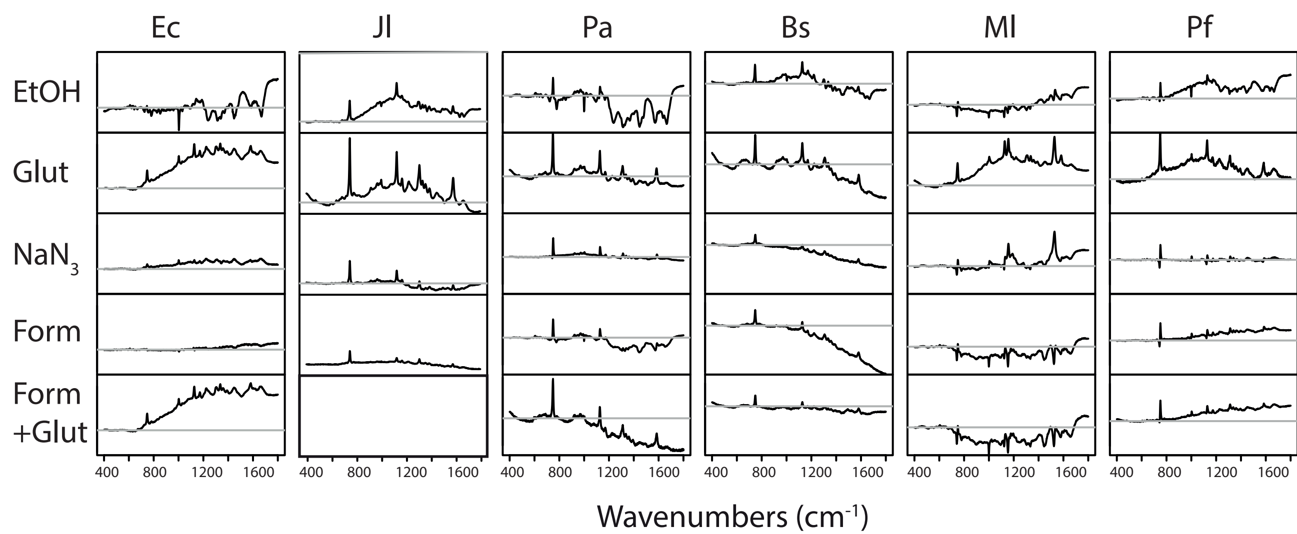

Ec
Jl
Pa
Bs
Ml
Pf
EtOH
Glut
NaN3
Form
Form +Glut
400
800
1200
1600
Wavenumbers (cm-1)

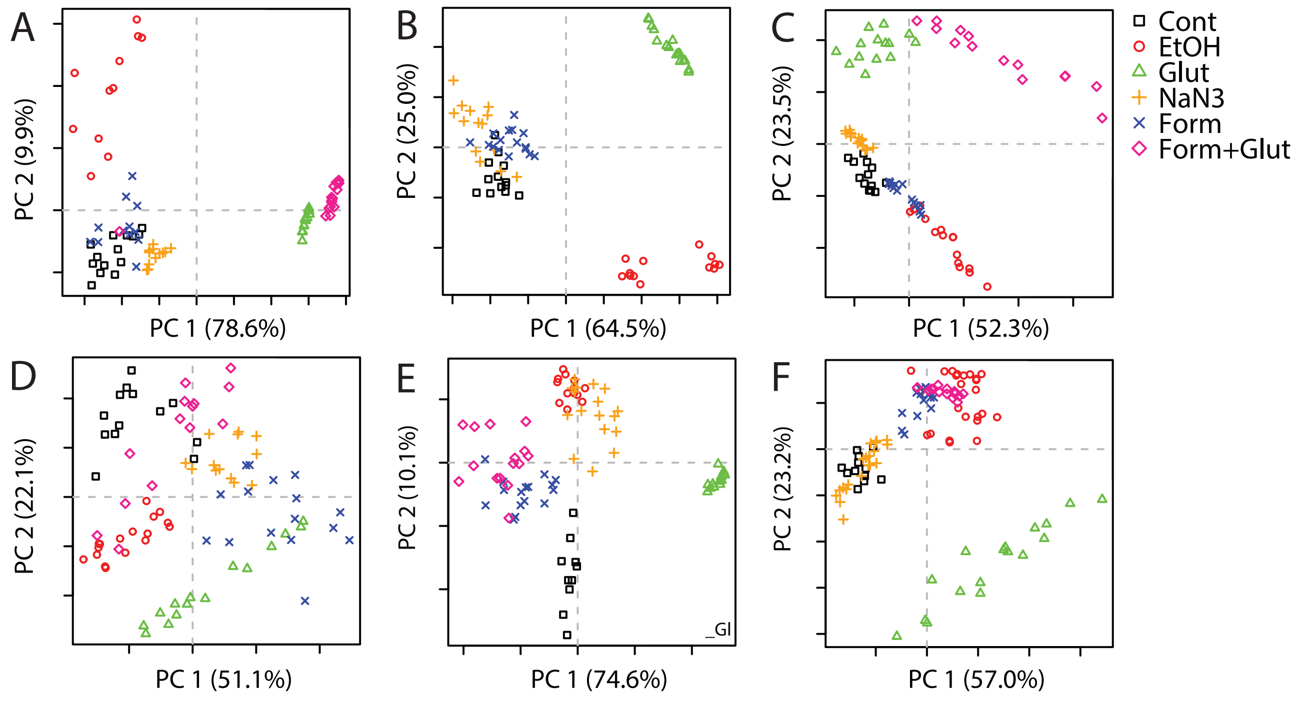
A
B
C
D
E
F
PC 1 (78.6%)
PC 2 (9.9%)
PC 1 (64.5%)
PC 2 (25.0%)
PC 1 (52.3%)
PC 2 (23.5%)
PC 1 (51.1%)
PC 2 (22.1%)
PC 1 (74.6%)
PC 2 (10.1%)
PC 1 (57.0%)
PC 2 (23.2%)
Cont
EtOH
Glut
NaN3
Form
Form+Glut

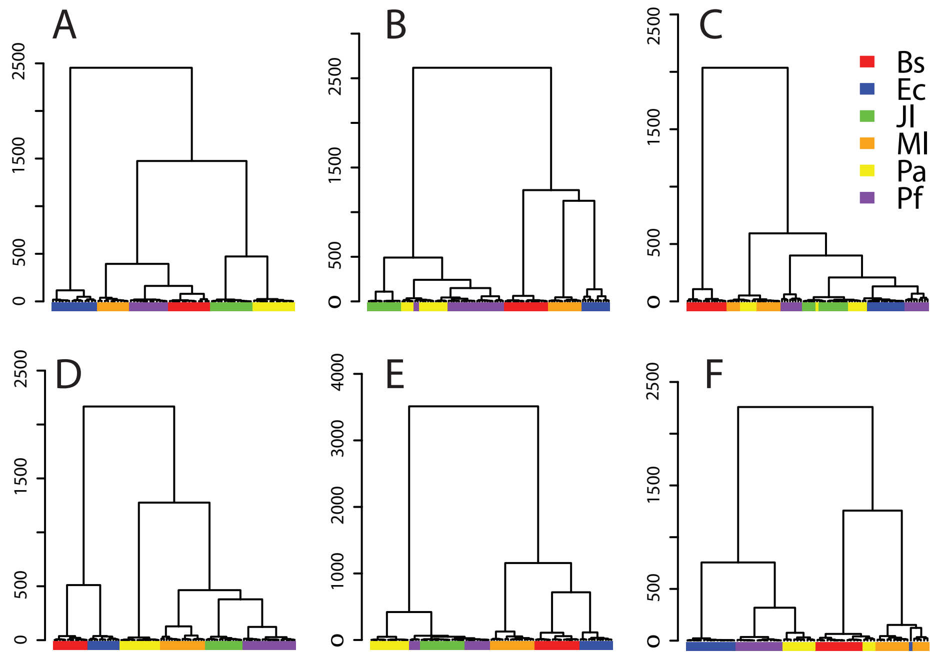
A
B
C
D
E
F
Bs
Ec
Jl
Ml
Pa
Pf